Influence of a laser field on Coulomb explosions and stopping power for swift molecular ions interacting with solids

Gui-Qiu Wang, Yuan-Hong Song, and You-Nian Wang*

The State Key Laboratory of Materials Modification by Laser, Electron, and Ion Beams, Department of Physics, Dalian University of Technology, Dalian 116023, People's Republic of China

Z. L. Mišković

Department of Applied Mathematics, University of Waterloo, Waterloo, Ontario, Canada N2L 3G1

(Received 19 February 2002; published 1 October 2002)

The influence of a high-intensity laser field on the inelastic interactions between a swift molecular ion and a solid target is studied by means of the dielectric theory. Excitations of the electron gas in the solid are described by the linearized hydrodynamic Poisson equations, thus allowing derivation of general expressions for the induced potential in the target and the interaction force among the ions within the molecule, in the presence of the laser field. Based on the numerical solution of the equations of motion for the constituent ions, the Coulomb explosion patterns and the molecular energy losses are discussed for a range of laser parameters.

DOI: 10.1103/PhysRevA.66.042901 PACS number(s): 79.20.Rf, 34.50.Bw

I. INTRODUCTION

The interactions of swift molecular and cluster ions with solids have been the subject of increasing interest during the past several decades. Soon after the observation of transmission of H_2^+ ions through carbon foils by Poizat and Remillieux [1], the first experimental demonstration and a theoretical description of the so-called vicinage effects in the energy loss of ion clusters were provided by Brandt *et al.* [2]. These effects originate from the interference among the electronic excitations of the solid arising from the correlated motion of the constituent ions in the cluster. Recent advances in experimental techniques have greatly stimulated further experimental and theoretical studies of various aspects of the interaction of large clusters with solids, such as Coulomb explosions and the energy losses [3–11]. A review of the current knowledge in the field of cluster-solid interactions has been published recently by Arista [12], where new developments of the theory were provided toward better description of the ion charge states within the clusters. In that context, a self-consistent theoretical model has been developed recently for the vicinage effects on the charge states of the constituent ions in clusters moving through solids [13,14]. Apart from the evident attraction of the cluster-solid interactions for researchers in the area of interactions of particles with matter, numerous applications of clusters in materials modification and fusion technology are being considered in the literature.

On the other hand, particle interactions with matter in the presence of a laser field have come into the focus of research in the past decade. For example, the interaction of charged particles with a plasma in the presence of a strong laser field has attracted much interest owing to the possibility of using fast and heavy ion beams as drivers in inertial confinement fusion experiments [15–18]. An ablated plasma has been created in recent experiments [19–22] by irradiation of a solid surface with a strong, pulsed laser beam, with simultaneous bombardment of the target surface by a heavy ion beam. It is expected in such experiments that the presence of the laser field will affect the energy loss of the ion beam, as a result of the modulation effects of the laser field on the motion of electrons in the target. On the theoretical side, a general formulation has been developed for describing the effects of a strong laser field on the stopping power of a swift ion, based on a time-dependent Hamiltonian for a degenerate free-electron gas in the presence of both the laser field and the self-consistent scalar electric field [23,24]. It has been found that the laser field can induce a decrease of the stopping power for intermediate-velocity ions, while an increase of the stopping power may occur at low velocities, due to a resonance process of plasmon excitations assisted by a photon absorption. Moreover, Nersisyan and Akopyan [25] found that charged particles may be accelerated by the laser field in the high-intensity limit. In addition, Zhang and Xu [26,27] have studied the effects of the laser field on the energy loss rate of charged particles moving in a two-dimensional electron gas by solving a time-dependent Schrödinger equation.

Although it is expected that the presence of a laser field may provide powerful means of controlling the interactions of clusters with matter, very few studies have been reported on such systems so far. For example, Silva and Galvão have recently studied the effects of the laser field on the energy loss of ion clusters moving in a hot plasma [28] and found that the laser field induces a decrease of the energy loss, when compared to the laser-free case. However, the Coulomb explosion effects of the cluster were not included in their work. In reality, when a fast cluster enters a solid target, it will be quickly stripped of its valence electrons, and further penetration of the resulting constituent ions will be accompanied by simultaneous processes of the Coulomb explosion and the energy deposition into the electron excitations

*Email address: ynwang@dlut.edu.cn

of the target. One expects therefore that, in general, the dispersion of the ion cluster due to the Coulomb explosion will diminish the vicinage effects on the energy losses. Moreover, the Coulomb explosion patterns of clusters show a strong asymmetry for prolonged penetration times, owing to the wake effects in the dynamic response of the target electron gas [29]. Further complications arise from the interplay between the vicinage effects on the ion charge states in the cluster, the energy losses, and the asymmetric Coulomb explosions. In this work, we present a study of the influence of a high-intensity laser field on the Coulomb explosions and energy losses of fast molecular ions in a solid target, based on an extension of the method used in our previous work [30], where the excitations of the electron gas in the target were described by the hydrodynamic model. We consider the constituent ions in the cluster to be pointlike perturbers with fixed charge, such as in the case of fast hydrogen clusters, leaving the problem of the vicinage effects on charge states in the presence of a laser field for future work.

The paper is organized as follows. In Sec. II, we use a Fourier-like analysis of the linearized hydrodynamic Poisson equations to derive general expressions for the dynamically screened interaction potential and the corresponding force among the constituent ions in a fast cluster in the presence of a laser field. In Sec. III, we study the effects of the laser field on the Coulomb explosion dynamics of the cluster by solving the equations of motion for the constituent ions. Finally, modifications of the laser-assisted energy losses of the cluster due to the Coulomb explosion are studied in Sec. IV for prolonged penetration depths. A brief summary of the results is presented in Sec. V. Atomic units (a.u.) are used throughout, unless otherwise indicated.

II. INTERACTION POTENTIAL

As in the previous work [30], the electron plasma in a solid can be regarded as a degenerate free-electron gas with a homogeneous density n_0. During the irradiation by a laser field the electron gas remains homogeneous to the lowest-order approximation and retains the unperturbed density n_0. Given the laser field $\mathbf{E}_L(t)=\mathbf{E}_0\sin(\omega_0 t)$, the velocity of the individual electrons in the electron gas can be expressed as

$$\mathbf{u}_0(t)=\frac{1}{\omega_0}\mathbf{E}_0\cos(\omega_0 t), \tag{1}$$

where $\mathbf{E}_0$ is the field amplitude and ω_0 is the laser frequency.

Now consider a point charge with the charge number Z_1 and the velocity $\mathbf{v}$, moving in the electron gas. The charge density of the projectile can be written as

$$\rho_{ext}(\mathbf{r},t)=Z_1\delta(\mathbf{r}-\mathbf{v}t). \tag{2}$$

As a result, the equilibrium state of the electron gas will be perturbed and electronic excitations will be induced around the ion. We consider the electron gas as a charged fluid with the velocity field $\mathbf{u}(\mathbf{r},t)$ and the density $n(\mathbf{r},t)$. Based on the hydrodynamic model [31,32], the electronic excitations in the fluid can be described by the continuity equation

$$\frac{\partial n}{\partial t}+\nabla\cdot(\mathbf{u}n)=0, \tag{3}$$

the momentum-balance equation

$$\frac{\partial \mathbf{u}}{\partial t}+(\mathbf{u}\cdot\nabla)\mathbf{u}=-\mathbf{E}_L(t)+\nabla\Phi(\mathbf{r},t)+\mathbf{F}_{int}+\mathbf{F}_f, \tag{4}$$

and Poisson's equation

$$\nabla^2\Phi=-4\pi[\rho_{ext}(\mathbf{r},t)+n_0-n]. \tag{5}$$

In Eq. (4), $\mathbf{E}_L(t)$ is the laser field, Φ is the scalar potential which results from the external charge ρ_{ext} and the charge-density polarization of the electron gas n_0-n, $\mathbf{F}_{int}$ is the internal interaction force of the fluid, which can be expressed by means of an energy functional $G[n]$, and $\mathbf{F}_f=-\gamma\mathbf{u}$ is the frictional force on electrons due to scattering on the positive-charge background, with γ being the friction coefficient, which is taken to be an infinitesimally small positive quantity.

According to the Thomas–Fermi–Dirac–von Weiszacker approximation [33,34], the energy functional $G[n]$ is defined by

$$G[n]=\int d\mathbf{r}\, n(\mathbf{r},t)\mathcal{E}(n,\nabla n) \tag{6}$$

in terms of the local internal energy per electron in the fluid,

$$\mathcal{E}(n,\nabla n)=\frac{3}{10}(3\pi^2 n)^{2/3}+\frac{1}{8}\frac{(\nabla n)^2}{n^2}, \tag{7}$$

where exchange and correlation contributions are neglected. It will be shown that the use of such a model for $\mathcal{E}(n,\nabla n)$ in the linearized equations yields the well-known plasmon-pole approximation (PPA) for the dielectric function of the electron gas. With the energy functional $G[n]$, the internal force $\mathbf{F}_{int}$ is given by

$$\mathbf{F}_{int}=-\nabla\left(\frac{\delta G}{\delta n}\right). \tag{8}$$

The system of Eqs. (3)–(8) constitutes a set of self-consistent nonlinear equations, which can only be solved numerically, in general. Since we are primarily interested in high-velocity molecular ions, one can consider the ion charge distribution ρ_{ext} as a weak, first-order perturbation of the electron fluid. We therefore linearize the above equations by retaining the laser field $\mathbf{E}_L(t)$ in the lowest-order approximation and assuming $n(\mathbf{r},t)=n_0+n_1(\mathbf{r},t)$ and $\mathbf{u}(\mathbf{r},t)$

$=\mathbf{u}_0(t)+\mathbf{u}_1(\mathbf{r},t)$, where $\mathbf{u}_0(t)$ is given by Eq. (1), while $n_1(\mathbf{r},t)$ and $\mathbf{u}_1(\mathbf{r},t)$ are the perturbed flow velocity and density, respectively. According to Eq. (5), the potential Φ will be therefore obtained as a perturbed quantity in the first-order approximation, which is equivalent to the linear-response treatment of the external charge in solids [23], or to the linearized Vlasov equation approach for plasmas [35], in the presence of a strong laser field. We further adopt the approach used in [35] and introduce translational shift to an oscillating frame of reference by means of the new variable $\mathbf{s}=\mathbf{r}-\mathbf{a}\sin(\omega_0 t)$, where $\mathbf{a}=\mathbf{E}_0/\omega_0^2$ is the transverse-oscillation amplitude of electrons driven by the laser field (the so-called quiver amplitude). As a result, we obtain the following linearized equations [30,31]:

$$\frac{\partial n_1}{\partial t}=-n_0\nabla_{\mathbf{s}}\cdot\mathbf{u}_1, \tag{9}$$

$$\frac{\partial \mathbf{u}_1}{\partial t}=\nabla_{\mathbf{s}}\Phi-\frac{v_F^2}{3n_0}\nabla_{\mathbf{s}}n_1+\frac{1}{4n_0}\nabla_{\mathbf{s}}(\nabla_{\mathbf{s}}^2 n_1)-\gamma\mathbf{u}_1,$$

$$\nabla_{\mathbf{s}}^2\Phi=4\pi[n_1-\rho_{ext}(\mathbf{s},t)],$$

where $\nabla_{\mathbf{s}}\equiv\partial/\partial\mathbf{s}$ and $\rho_{ext}(\mathbf{s},t)=Z_1\delta[\mathbf{s}-\mathbf{v}t+\mathbf{a}\sin(\omega_0 t)]$ is the external charge in the shifted frame, while $v_F=(3\pi^2 n_0)^{1/3}$ is the Fermi velocity of the electron gas. The first term on the right-hand side of the momentum-balance equation is associated with the perturbed electric force, while the other terms are due to the internal interaction force of the electron gas and the frictional force [30].

We further apply the Fourier transform [23,30,35]

$$A(\mathbf{s},t)=\int\int\frac{d\mathbf{k}\,d\omega}{(2\pi)^4}A(\mathbf{k},\omega)e^{i\mathbf{k}\cdot\mathbf{s}-i\omega t}, \tag{10}$$

where $A(\mathbf{s},t)$ stands for any of the above listed perturbed quantities in the shifted frame of reference. With this transform, the scalar potential is readily obtained as follows:

$$\Phi(\mathbf{k},\omega)=\frac{4\pi\rho_{ext}(\mathbf{k},\omega)}{k^2\varepsilon(k,\omega)}, \tag{11}$$

where the resulting dielectric function $\varepsilon(k,\omega)$ has the form corresponding to the so-called plasmon-pole approximation, viz.,

$$\varepsilon(k,\omega)=1-\frac{\omega_p^2}{\omega(\omega+i\gamma)-(v_F^2k^2/3+k^4/4)}, \tag{12}$$

which is commonly employed in the literature to describe the dielectric response to fast ions, with $\omega_p=\sqrt{4\pi n_0}$ being the plasma frequency. This form of the dielectric function is the consequence of the model used for the energy functional based on the Thomas–Fermi–Dirac–von Weiszacker approximation [31,32]. In Eq. (11), $\rho_{ext}(\mathbf{k},\omega)=Z_1\int dt\exp[-i\mathbf{k}\cdot\mathbf{a}\sin(\omega_0 t)+i(\omega-\mathbf{k}\cdot\mathbf{v})t]$ is the Fourier transform of the external charge density $\rho_{ext}(\mathbf{s},t)$. On using the Jacobi identity, $\exp[i\mathbf{k}\cdot\mathbf{a}\sin(\omega_0 t)]=\Sigma J_n(\mathbf{k}\cdot\mathbf{a})\exp(i\omega_0 t)$, we obtain

$$\rho_{ext}(\mathbf{k},\omega)=2\pi Z_1\sum_{n=-\infty}^{\infty}J_n(\mathbf{k}\cdot\mathbf{a})\,\delta(\omega+n\omega_0-\mathbf{k}\cdot\mathbf{v}), \tag{13}$$

where $J_n(x)$ is the nth-order Bessel function of the first kind. With Eqs. (11) and (13), the scalar potential can be written as

$$\Phi(\mathbf{r},t)=\sum_{n,m}\frac{Z_1}{2\pi^2}\int\frac{d\mathbf{k}}{k^2}J_m(\mathbf{k}\cdot\mathbf{a})J_n(\mathbf{k}\cdot\mathbf{a})\frac{e^{i\mathbf{k}\cdot(\mathbf{r}-\mathbf{v}t)}e^{i(n-m)\omega_0 t}}{\varepsilon(k,\omega_n)}, \tag{14}$$

where $\omega_n=\mathbf{k}\cdot\mathbf{v}-n\omega_0$ is the laser-harmonic Doppler-shifted frequency.

Next consider a fast homonuclear diatomic molecular ion moving in the electron gas. The interaction potential among the two constituent ions located at $\mathbf{r}_1$ and $\mathbf{r}_2$ is expressed as

$$U(\mathbf{r},t)=\int d\mathbf{r}'\rho_{ext}(\mathbf{r}'-\mathbf{r}_1,t)\Phi(\mathbf{r}'-\mathbf{r}_2,t)$$
$$=\sum_{n,m}\frac{Z_1^2}{2\pi^2}\int\frac{d\mathbf{k}}{k^2}J_m(\mathbf{k}\cdot\mathbf{a})J_n(\mathbf{k}\cdot\mathbf{a})\frac{e^{i\mathbf{k}\cdot\mathbf{r}}e^{i(n-m)\omega_0 t}}{\varepsilon(k,\omega_n)}, \tag{15}$$

where $\mathbf{r}=\mathbf{r}_1-\mathbf{r}_2$ is the relative position vector. After taking the time average over the laser period in this expression, the fast oscillations with time t are removed by setting the factor $e^{i(n-m)\omega_0 t}$ to zero unless $m=n$. As a result, the average interaction potential becomes time independent, viz.,

$$U(\mathbf{r})=\frac{Z_1^2}{2\pi^2}\sum_{n=-\infty}^{\infty}\int\frac{d\mathbf{k}}{k^2}\frac{J_n^2(\mathbf{k}\cdot\mathbf{a})e^{i\mathbf{k}\cdot\mathbf{r}}}{\varepsilon(k,\omega_n)}. \tag{16}$$

In order to simplify the following calculations, we assume that the three vectors $\mathbf{E}_0$, $\mathbf{v}$, and $\mathbf{k}$, are all in the same plane and take α to be the angle between $\mathbf{E}_0$ and $\mathbf{v}$. On introducing the variable $\omega=\mathbf{k}\cdot\mathbf{v}=kv\cos\theta$, we define the quantity

$$\chi(\kappa,\omega)=\mathbf{k}\cdot\mathbf{a}=\frac{a\omega}{v}\cos\alpha-\kappa a\sin\alpha, \tag{17}$$

with $\kappa=\sqrt{k^2-\omega^2/v^2}$. Assuming that the projectile velocity is directed along the z axis, the interaction potential can be written in the cylindrical coordinates $\mathbf{r}=(\boldsymbol{\rho},z)$ as follows:

$$U(\rho,z)=\frac{Z_1^2}{\pi v}\sum_{n=-\infty}^{\infty}\int_0^{\infty}\kappa d\kappa J_0(\kappa\rho)G_n(\kappa,z), \tag{18}$$

where

$$G_n(\kappa,z)=\int_{-\infty}^{\infty}\frac{d\omega}{\kappa^2+\omega^2/v^2}\frac{J_n^2(\chi(\kappa,\omega))}{\varepsilon(k,\omega-n\omega_0)}e^{i\omega z/v}. \quad (19)$$

It is clear that the interaction potential depends on the dielectric function of the target. In general, it is rather difficult to complete the integration in Eq. (19) if one uses the PPA dielectric function given by Eq. (12). However, in the high-velocity regime ($v \gg v_F$), the PPA dielectric function may be replaced by a local dielectric function

$$\varepsilon(k,\omega)=1-\frac{\omega_P^2}{\omega(\omega+i\gamma)}\Theta(k_{\max}-k), \quad (20)$$

where $k_{\max}=\omega_p/v_F$ is the cutoff wave number and Θ is the Heaviside step function. With such a simple dielectric function, one can carry out the integration in Eq. (19) by using the residue theorem. On introducing the screening length $\lambda_p=v/\omega_p$ and the dimensionless parameter $\sigma=\gamma/(2\omega_p)$, the interaction potential is finally expressed as

$$U(\rho,z)=U_D(\rho,z)+U_W(\rho,z), \quad (21)$$

where $U_D(\rho,z)$ is the well-known screened Coulomb potential

$$U_D(\rho,z)=\frac{Z_1^2}{r}-\frac{Z_1^2}{\lambda_p}\int_0^{\infty}d\kappa\, J_0(\kappa\rho/\lambda_p)G_D(\kappa)e^{-\kappa|z|/\lambda_p}, \quad (22)$$

while $U_W(\rho,z)$ is the asymmetric wake potential

$$U_W(\rho,z)=\frac{Z_1^2}{\lambda_p}\int_0^{v/v_F}\kappa\, d\kappa\, J_0(\kappa\rho/\lambda_p)G_W(\kappa,z) \times e^{-\sigma|z|/\lambda_p}\Theta(-z), \quad (23)$$

which results from the asymmetric dynamical polarizations in the medium. The functions $G_D(\kappa)$ and $G_W(\kappa,z)$ appearing in Eqs. (22) and (23) are given by

$$G_D(\kappa)=\frac{J_0^2(\chi(\kappa,0))}{\kappa^2+1}+2\sum_{n=1}^{\infty}\frac{\kappa^2+1-(n\beta)^2}{[\kappa^2+1-(n\beta)^2]^2+(2n\beta\kappa)^2} \times J_n^2(\chi(\kappa,0)) \quad (24)$$

and

$$G_W(\kappa,z)=\frac{1}{2(\kappa^2+1)}\{J_0^2(\chi(\kappa,1))+J_0^2(\chi(\kappa,-1))\}\sin(z/\lambda_p)+\frac{1}{2}\sum_{n=1}^{\infty}\frac{\{J_n^2(\chi(\kappa,n\beta+1))+J_n^2(\chi(\kappa,-n\beta-1))\}}{\kappa^2+(n\beta+1)^2} \times\sin[(n\beta+1)z/\lambda_p]-\frac{1}{2}\sum_{n=1}^{\infty}\frac{\{J_n^2(\chi(\kappa,n\beta-1))+J_n^2(\chi(\kappa,-n\beta+1))\}}{\kappa^2+(n\beta-1)^2}\sin[(n\beta-1)z/\lambda_p], \quad (25)$$

where $\beta=\omega_0/\omega_p$ is the reduced laser frequency, while $\chi(\kappa,n)=(a/\lambda_p)(n\cos\alpha-\kappa\sin\alpha)$. Obviously, U_W oscillates with z and exists only when $z<0$.

Finally, we study the variation of the interaction potential U with the longitudinal distance z for two point charges with $Z_1=1$, moving through an aluminum target at the speed $v=3$, in which the electron gas parameters are determined by $\omega_p=0.5749$, $\gamma=0.616\omega_p$, and $v_F=0.92$ [23,30]. Figures 1(a)–1(c) show the effects of the laser field on the potential for various laser-field intensities, frequencies, and angles between the laser field and the ion velocity, respectively. One observes that the amplitudes of oscillations in the potential decrease with increasing laser-field intensity, while the influences of both the frequency and the angle of the laser field on the potential are rather weak. In addition, the dependence of the potential on the coordinate z is rather asymmetric, as a direct consequence of the wake effects that reflect the oscillatory spatial pattern of the medium response.

III. COULOMB EXPLOSIONS

We consider here the influence of the laser field on the Coulomb explosion dynamics of a swift homonuclear diatomic molecular ion, moving through a solid with an initial velocity **v** along the direction of the z axis. During the penetration, the molecular ion dissociates into a cluster composed of two ions. The Coulomb explosion patterns can be described by solving the equations of motion for individual ions within the cluster. Thus, for the jth ion, one has

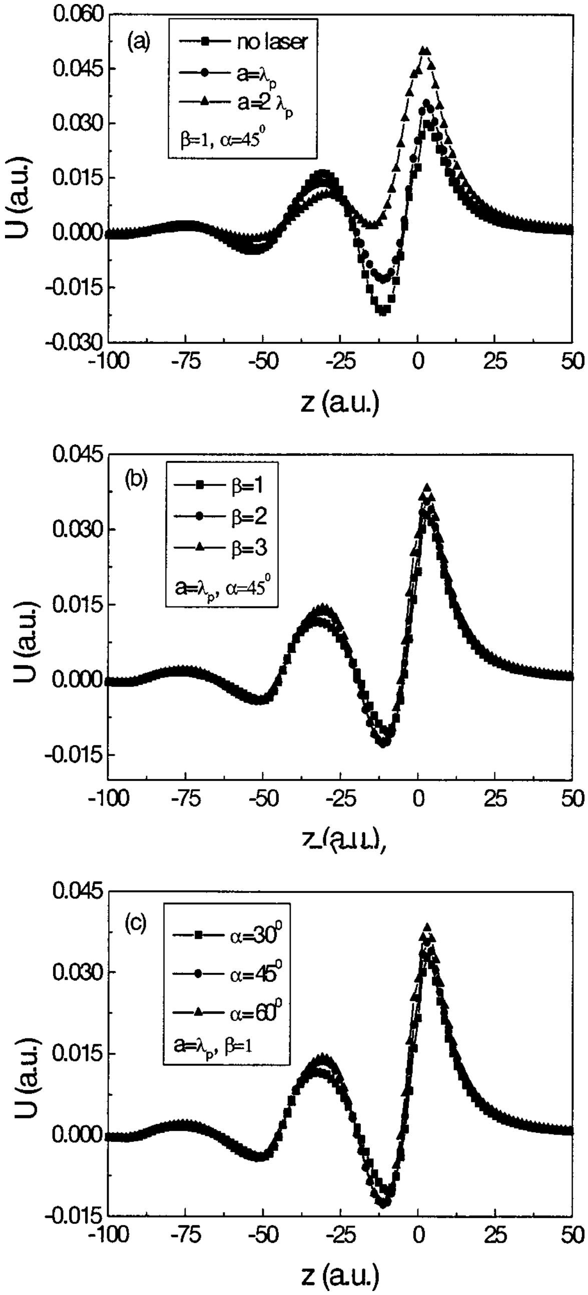

FIG. 1. Influence of (a) the laser intensity (i.e., the quiver amplitude) $a=E_0/\omega_0^2$, (b) the reduced laser frequency $\beta=\omega_0/\omega_p$, and (c) the laser-field angle α on the interaction potential U as a function of the longitudinal distance z, for two protons moving at the transversal distance $\rho=\lambda_p$ with the speed $v=3$ through an Al target.

$$m\frac{d^2\mathbf{r}_j}{dt^2}=\mathbf{F}_j^s+\sum_{j\neq l=1}^{2}\mathbf{F}(\mathbf{r}_{jl}), \tag{26}$$

where m is the ion mass, $\mathbf{F}_j^s=-\partial U(\mathbf{r}_{jl})/\partial\mathbf{r}_{jl}|_{\mathbf{r}_{jl}=0}$ is the self-stopping force, and the interaction force is given by $\mathbf{F}_{jl}=-\partial U(\mathbf{r}_{jl})/\partial\mathbf{r}_{jl}$, for $j\neq l$.

Since the velocities $\mathbf{v}_j$ of the individual ions change only slightly during the passage, we may assume that the velocities $\mathbf{v}_j$ are approximately equal to the initial velocity $\mathbf{v}$ in those expressions of the preceding section which are used to evaluate the forces in Eq. (26). Thus, the self-stopping force depends only on the velocity $\mathbf{v}$, i.e., $\mathbf{F}_1^s=\mathbf{F}_2^s=F^s(v)\mathbf{e}_z$, where

$$F_s(v)=-\frac{Z_1^2}{\lambda_p^2}\int_0^{v/v_F}\kappa\, d\kappa\, G(\kappa), \tag{27}$$

with

$$\begin{aligned}G(\kappa)=&\frac{\{J_0^2(\chi(\kappa,1))+J_0^2(\chi(\kappa,-1))\}}{2(\kappa^2+1)}\\&+\frac{1}{2}\sum_{n=1}^{\infty}\frac{\{J_n^2(\chi(\kappa,n\beta+1))+J_n^2(\chi(\kappa,-n\beta-1))\}}{\kappa^2+(n\beta+1)^2}\\&-\frac{1}{2}\sum_{n=1}^{\infty}\frac{\{J_n^2(\chi(\kappa,n\beta-1))+J_n^2(\chi(\kappa,-n\beta+1))\}}{\kappa^2+(n\beta-1)^2}.\end{aligned} \tag{28}$$

In analogy to the interaction potential, the interaction force $\mathbf{F}$ can also be decomposed into two parts, i.e., $\mathbf{F}=\mathbf{F}_D+\mathbf{F}_W$, where $\mathbf{F}_D$ is the screened Coulomb force and $\mathbf{F}_W$ is the wake force. On using the expressions for the interionic potential from the preceding section, one obtains the components of $\mathbf{F}_D$ and $\mathbf{F}_W$ in the xz plane as follows:

$$\begin{aligned}F_{Dx}(x,z)=&\frac{Z_1^2}{\lambda_p^2}\frac{x}{r^3}-\frac{Z_1^2}{\lambda_p^2}\frac{x}{|x|}\int_0^{\infty}\kappa\, d\kappa\, J_1(\kappa|x|/\lambda_D)G_D(\kappa)\\&\times e^{-\kappa|z|/\lambda_D},\end{aligned} \tag{29}$$

$$\begin{aligned}F_{Dz}(x,z)=&\frac{Z_1^2}{\lambda_p^2}\frac{z}{r^3}-\frac{Z_1^2}{\lambda_p^2}\frac{z}{|z|}\int_0^{\infty}\kappa\, d\kappa\, J_0(\kappa|x|/\lambda_D)G_D(\kappa)\\&\times e^{-\kappa|z|/\lambda_D},\end{aligned} \tag{30}$$

$$\begin{aligned}F_{Wx}(x,z)=&\frac{Z_1^2}{\lambda_p^2}\frac{x}{|x|}\int_0^{v/v_F}\kappa^2\, d\kappa\, J_1(\kappa|x|/\lambda_D)\\&\times G_W(\kappa,z)e^{-\alpha|Z|/\lambda_D}\Theta(-z),\end{aligned} \tag{31}$$

$$\begin{aligned}F_{Wz}(x,z)=&-\frac{Z_1^2}{\lambda_p^2}\int_0^{v/v_F}\kappa\, d\kappa\, J_0(\kappa|x|/\lambda_D)\\&\times G_W^{(1)}(\kappa,z)e^{-\alpha|Z|/\lambda_D}\Theta(-z),\end{aligned} \tag{32}$$

where

$$G_W^{(1)}(\kappa,z)=\frac{\{J_0^2(\chi(\kappa,1))+J_0^2(\chi(\kappa,-1))\}}{2(\kappa^2+1)}[\cos(z/\lambda_D)+\sigma\sin(z/\lambda_D)]$$
$$+\frac{1}{2}\sum_{n=1}^{\infty}\frac{\{J_n^2(\chi(\kappa,n\beta+1))+J_n^2(\chi(\kappa,-n\beta-1))\}}{\kappa^2+(n\beta+1)^2}\{(n\beta+1)\cos[(n\beta+1)z/\lambda_D]+\sigma\sin[(n\beta+1)z/\lambda_D]\}$$
$$-\frac{1}{2}\sum_{n=1}^{\infty}\frac{\{J_n^2(\chi(\kappa,n\beta-1))+J_n^2(\chi(\kappa,-n\beta+1))\}}{\kappa^2+(n\beta-1)^2}\{(n\beta-1)\cos[(n\beta-1)z/\lambda_D]-\sigma\sin[(n\beta-1)z/\lambda_D]\}. \tag{33}$$

The influence of the laser-field parameters on the longitudinal F_z and transversal F_x components of the total force are shown in Figs. 2(a)–2(c) and Figs. 3(a)–3(c), respectively, in a manner similar to that in Fig. 1(a)–1(c).

It is convenient to study the Coulomb explosion dynamics of the diatomic molecule in terms of the relative position $\mathbf{r}=\mathbf{r}_1-\mathbf{r}_2$ and the relative velocity $\mathbf{w}=\mathbf{v}_1-\mathbf{v}_2$. Thus, the equations for the relative motion are

$$\frac{d\mathbf{r}}{dt}=\mathbf{w}, \tag{34}$$

$$\frac{d\mathbf{w}}{dt}=\frac{1}{m}[\mathbf{F}(\mathbf{r})-\mathbf{F}(-\mathbf{r})]. \tag{35}$$

Finally, the equations for the components of the relative position and the relative velocity in the xz plane are

$$dx/dD=w_x/v, \tag{36}$$

$$dz/dD=w_z/v,$$

$$dw_x/dD=\frac{1}{mv}[2F_{Dx}(x,z)+F_{Wx}(x,z)-F_{Wx}(-x,-z)],$$

$$dw_z/dD=\frac{1}{mv}[2F_{Dz}(x,z)+F_{Wz}(x,z)-F_{Wz}(-x,-z)],$$

where $D=vt$ is the penetration depth.

Equations (36) provide a self-consistent procedure to determine the influence of the laser field on the Coulomb explosion dynamics of a swift dicluster. In the xz plane, the initial relative position of the two ions in H_2^+ can be expressed as $\mathbf{r}_0=(r_0\sin\zeta_0, r_0\cos\zeta_0)$, where $r_0=1.06$ a.u. is the initial internuclear distance and ζ_0 is the initial azimuthal angle ranging from $-\pi/2$ to $\pi/2$. In addition, the initial relative velocity $\mathbf{w}_0$ is zero, allowing Eqs. (36) to be solved numerically with the appropriate initial conditions. In the following calculations, we assume the initial angle $\zeta_0=60°$.

We consider first how the direction of the molecular axis changes during the Coulomb explosion under the influence of a strong laser field. We plot in Figs. 4(a)–4(c) the angle ζ between the molecular axis and the beam direction as a function of the penetration depth D for various laser parameters. One can see from these figures that the molecular axis tends to align itself with the beam direction during penetration for all sets of the laser parameters displayed. In particular, we notice that the angle ζ changes more slowly for larger laser intensity. On the other hand, our computations showed that the laser-field parameters have very little influence on the increase of the internuclear distance r in the course of a Coulomb explosion. In Figs. 5(a)–5(b), we plot the dependences of the angle ζ and the distance r, respectively, on the penetration depth D for different molecule speeds in the laser field characterized by $a=\lambda_p$, $\beta=1$, and $\alpha=45°$.

IV. STOPPING POWER

On using Eq. (26), one can obtain the expression for the stopping power of the molecular ion [36] in the following form:

$$S_{mol}=2S_p(v)+S_v(x,z,v), \tag{37}$$

where $S_p(v)=-F_s(v)$ is the proton stopping power, while $S_v(x,z,v)=-F_{Wz}(x,z,v)-F_{Wz}(-x,-z,v)$ is the vicinage stopping power. The first term on the right-hand side of Eq. (37) gives the laser-assisted stopping power for two uncorrelated ions, while the second term results from the correlated motion of the two ions in the cluster. We note that, upon solving the equations for the relative motion of ions during the Coulomb explosion, the components x and z of the interionic separation become functions of the penetration depth D, and so does the vicinage stopping power $S_v(x,z,v)$.

Figures 6(a)–6(c) show the stopping power of the dicluster with $Z_1=1$ as a function of the penetration depth D for different laser parameters. In general, the stopping power decreases with increasing depth D for all sets of laser parameters displayed, thus reflecting the diminishing vicinage effects on the molecular energy loss in the course of the Cou-

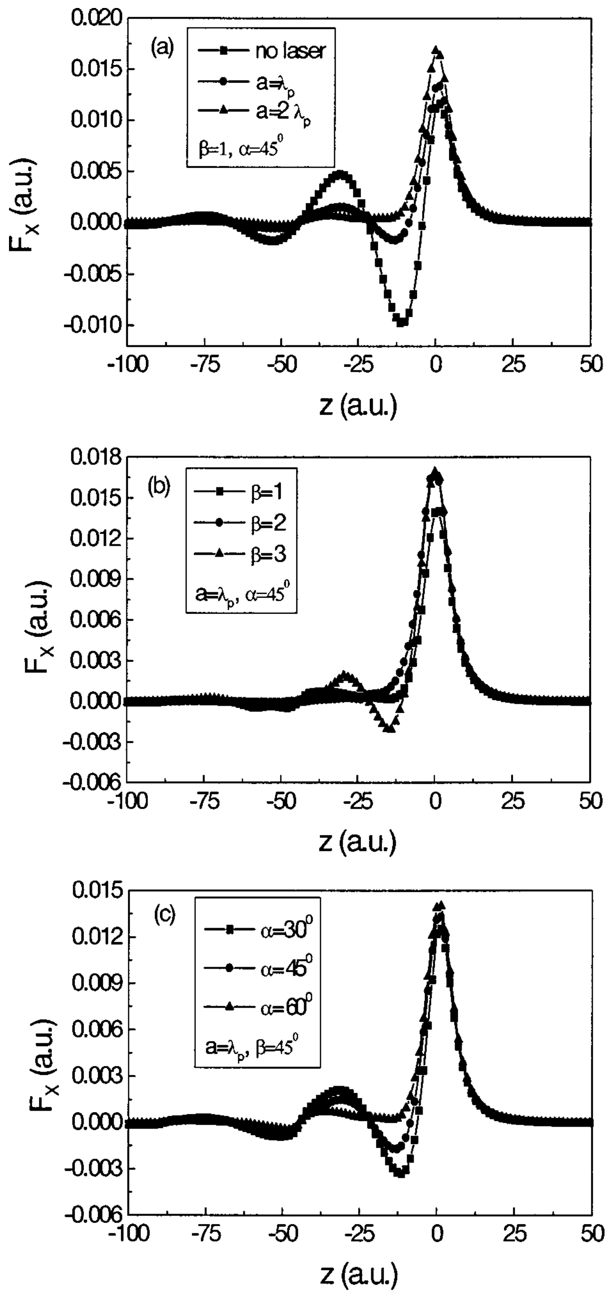

FIG. 2. Influence of (a) the laser intensity (i.e., the quiver amplitude) $a=E_0/\omega_0^2$, (b) the reduced laser frequency $\beta=\omega_0/\omega_p$, and (c) the laser-field angle α on the transversal component F_x of the interaction force as a function of the longitudinal distance z, for two protons moving at the transversal distance $\rho=\lambda_p$ with the speed $v=3$ through an Al target.

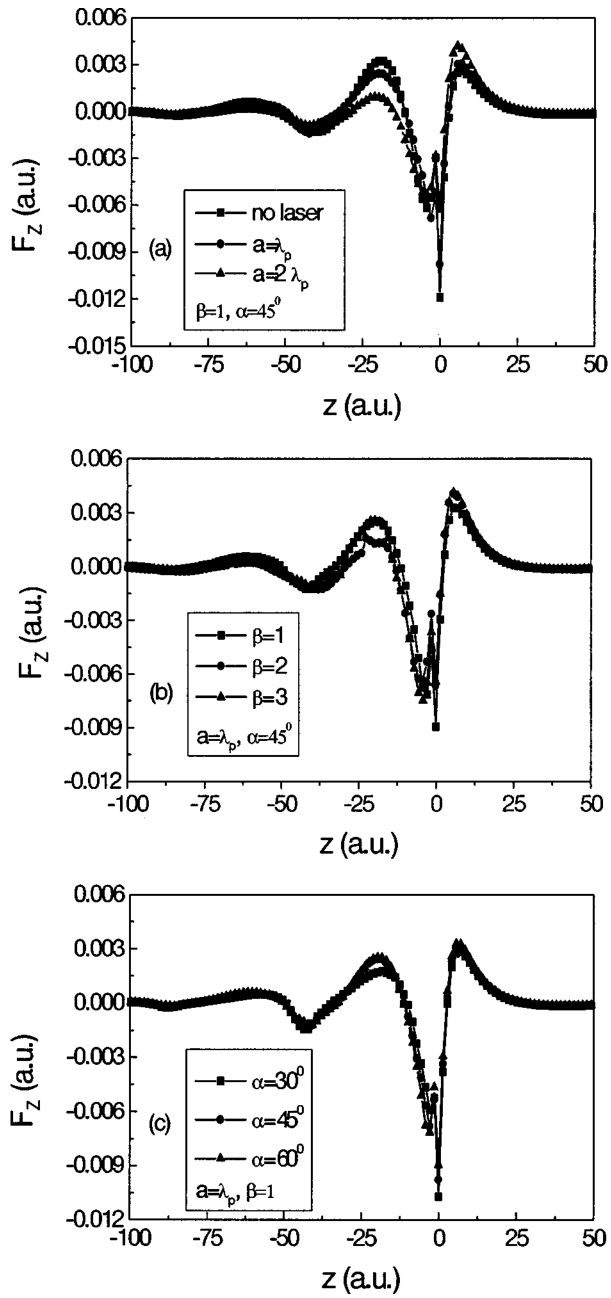

FIG. 3. Influence of (a) the laser intensity (i.e., the quiver amplitude) $a=E_0/\omega_0^2$, (b) the reduced laser frequency $\beta=\omega_0/\omega_p$, and (c) the laser-field angle α on the longitudinal component F_z of the interaction force as a function of the longitudinal distance z, for two protons moving at the transversal distance $\rho=\lambda_p$ with the speed $v=3$ through an Al target.

lomb explosion. In particular, one can see in Fig. 6(a) that the magnitude of the stopping power decreases significantly with increasing laser intensity at all depths D. This indicates that the conclusions drawn in the previous work [28,30] that variable laser intensity can be used to modulate the stopping power of both the molecular and atomic ions, may be extended into the regime where the molecular energy losses are modified by the Coulomb explosion. On the other hand, the data shown in Figs. 6(b) and 6(c) exhibit no systematic trends regarding the dependence of the stopping power on either the frequency ratio β or the angle α, which is probably due to a complicated superposition of the oscillations of trigonometric functions with β and α in the expressions derived in the preceding sections.

In order to further clarify the role of Coulomb explosion in diminishing vicinage effects on molecular energy loss, we show in Figs. 7(a)–7(c) the stopping power ratio $R=1+S_v(x,z,v)/2S_p(v)$ as a function of the penetration depth D, for different laser parameters. One can see that the stopping

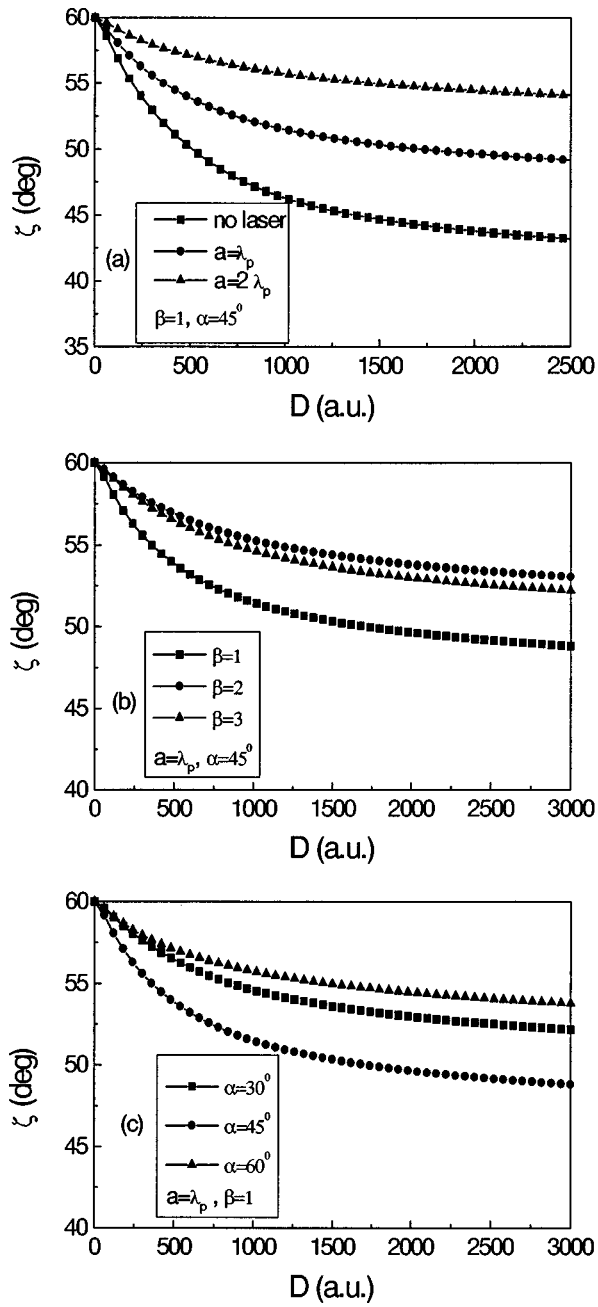

FIG. 4. The dependence of the angle ζ between the molecular axis and the beam direction as a function of the penetration depth D on (a) the laser intensity a (with $\beta=1$ and $\alpha=45\,°$), (b) the laser frequency β (with $a=\lambda_p$ and $\alpha=45\,°$), and (c) the laser-beam angle α (with $a=\lambda_p$ and $\beta=1$), during the Coulomb explosion of a hydrogen molecular ion moving through an Al target with the speed $v=3$ and the initial angle $\zeta_0=60\,°$.

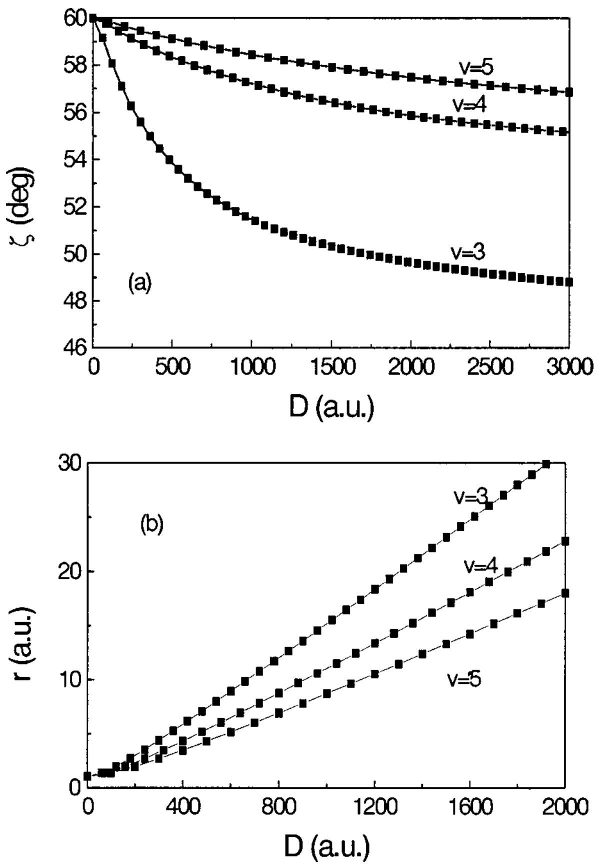

FIG. 5. The dependence of (a) the molecular axis angle ζ and (b) the internuclear distance r on the penetration depth D during the Coulomb explosion of a hydrogen molecular ion moving through an Al target at several speeds $v=3$, 4, and 5, with the initial angle $\zeta_0=60\,°$, in the presence of a laser field with the parameters $a=\lambda_p$, $\beta=1$, and $\alpha=45\,°$.

power ratio is close to 2 at the beginning of the penetration, when the two constituent ions are so close to each other that they act as if they were almost united into a single pointlike projectile with the double charge. For prolonged penetration depths D, the stopping ratio R approaches 1, indicating that the two ions have moved away from each other in the course of Coulomb explosion to sufficiently large separations that they act as two completely independent or uncorrelated perturbers of the electron gas. It is interesting to note, however, that the influence of the different laser-parameter regimes on the stopping ratio dependence on D, shown in Figs. 7(a)–7(c), is not particularly strong. This seems to be related to our observation in the preceding section that the increase of the interionic distance during the Coulomb explosion is only weakly influenced by the laser-field parameters while, at the same time, the vicinage effects on the molecular energy loss appear to be influenced more by the interionic distances than by the orientation of the molecular axis.

Finally, we display the influence of the projectile speed v on the stopping power S_{mol} and the stopping ratio R in Figs. 8(a)–8(b), respectively, for fixed laser parameters. Figure 8(a) shows clearly that, for a fixed penetration depth D, the magnitude of the molecular stopping power decreases as the projectile velocity increases. On the other hand, Fig. 8(b) suggests that the rate of decrease of the stopping ratio R with increasing penetration depth D is strongly influenced by the speed. Even though the differences among the curves shown in Fig. 8(b) would be somewhat smaller if they were replotted against the dwell time $t=D/v$ rather than the depth D, the residual differences would still indicate a strong role of the molecule speed in the decrease of the stopping ratio with increasing penetration time.

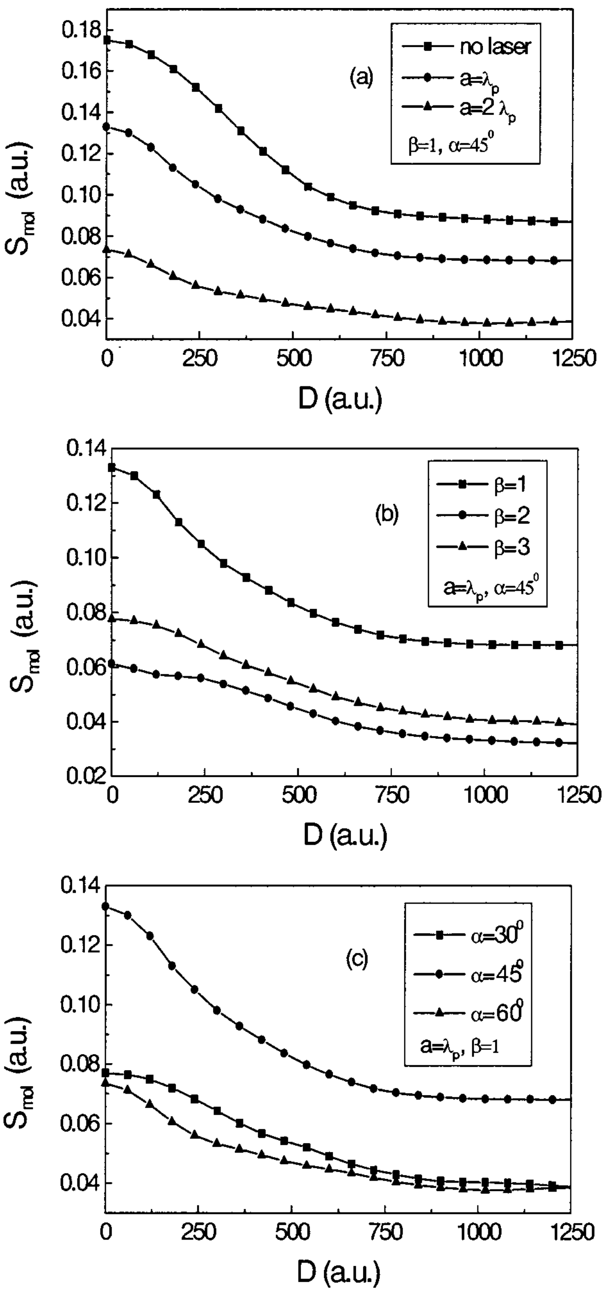

FIG. 6. Influence of (a) the laser intensity a (with $\beta=1$ and $\alpha=45°$), (b) the laser frequency β (with $a=\lambda_p$ and $\alpha=45°$), and (c) the laser-beam angle α (with $a=\lambda_p$ and $\beta=1$), on the molecular stopping power S_{mol} as a function of the penetration distance D, during the Coulomb explosion of a hydrogen molecular ion moving through an Al target with the speed $v=3$ and the initial angle $\zeta_0=60°$.

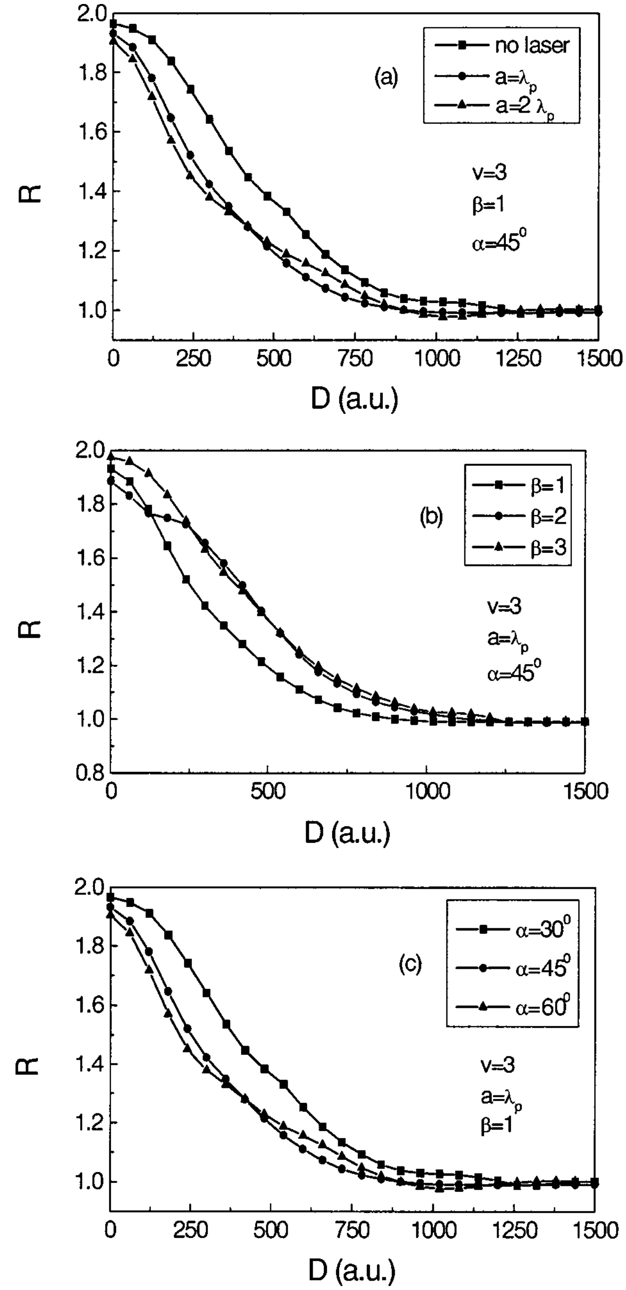

FIG. 7. Influence of (a) the laser intensity a (with $\beta=1$ and $\alpha=45°$), (b) the laser frequency β (with $a=\lambda_p$ and $\alpha=45°$), and (c) the laser-beam angle α (with $a=\lambda_p$ and $\beta=1$), on the stopping-power ratio R as a function of the penetration distance D, during the Coulomb explosion of a hydrogen molecular ion moving through an Al target with the speed $v=3$ and the initial angle $\zeta_0=60°$.

V. SUMMARY

We have used the linearized hydrodynamic Poisson equations to describe the excitations of the electron gas in a solid target in the presence of a high-intensity laser field, caused by the passage of a swift diatomic molecular ion. In particular, we have focused on the laser-field effects on the dynamically screened interionic interaction governing the Coulomb explosion of the molecule which, in turn, is responsible for weakening of the vicinage effects on the molecular energy loss with increasing dwell time through the target.

General expressions for the interaction potential among the two constituent ions have been derived by means of a Fourier-like transform, in conjunction with a simple local dielectric function, which is appropriate for collective excitations of the electron gas. The potential (force) among the two ions has been divided into two parts: the symmetrically screened Coulomb potential (force) and the asymmetric wake potential (force). The former describes a repulsive

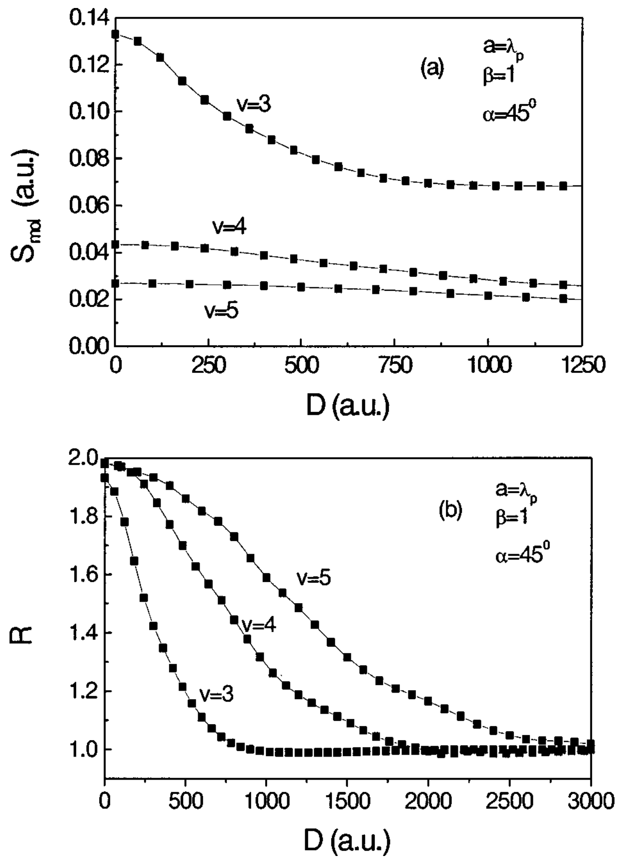

FIG. 8. The dependence of (a) the stopping power S_{mol} and (b) the stopping power ratio R on the penetration depth D during the Coulomb explosion of a hydrogen molecular ion moving through an Al target at several speeds $v=3$, 4, and 5, with the initial angle $\zeta_0=60°$, in the presence of a laser field with the parameters $a=\lambda_p$, $\beta=1$, and $\alpha=45°$.

interaction which decreases very quickly with increasing interionic distance, while the latter describes an oscillatory, long-range asymmetric interaction. Numerical results show that the laser-field intensity is an important parameter affecting the interaction among the ions, in such a manner that the amplitude of oscillations of the wake potential (force) decreases with increasing laser-field intensity.

Furthermore, using the results for the total interaction force, we have numerically solved the equations of motion for the two ions, in order to reveal the effects of the laser field on the Coulomb explosion dynamics and the molecular stopping power. It has been found that, due to the wake effects, the molecular axis tends to align itself along the beam direction with increasing penetrating depth, but this tendency is significantly reduced by increasing the laser-field intensity. On the other hand, the laser-field intensity has little effect on the increase of the interionic distance during the course of Coulomb explosion.

Finally, using the results for the relative motion of the two constituent ions during the Coulomb explosion, we have found that, generally, in the presence of a laser field, the magnitude of the molecular stopping power decreases with increasing penetration depth, due to weakening of the constructive interference in the electron-gas excitations with increasing interionic distance. While increasing laser-field intensity has been found to strongly suppress the stopping power magnitude for all penetration depths, the other laser-field parameters do not show any appreciably systematic effects. Somewhat surprisingly, the relative effect of the laser field on the decrease of stopping power with increasing depth, expressed via the stopping power ratio, exhibits very little influence of the laser-field parameters, which can be ascribed to the fact that the increase of the interionic distance during the Coulomb explosion is rather insensitive to the presence of the laser field.

The results obtained in the present work may be helpful in further studies dedicated to using various parameters of a laser field to control the rate of energy deposition of fast molecular and cluster ions in a plasma ablated by a laser field.

ACKNOWLEDGMENTS

This work is jointly supported by the National Natural Science Foundation of China (Grant No. 19975008) and a Grant for Cross-Century Excellent Scholar of the Ministry of Education State of China.

[1] J. C. Poizat and J. Remillieux, Phys. Lett. **34A**, 53 (1971).
[2] W. Brandt, A. Ratkowsky, and R. H. Ritchie, Phys. Rev. Lett. **33**, 1325 (1974).
[3] N. R. Arista and V. H. Ponce, J. Phys. C **8**, L188 (1975).
[4] N. R. Arista, Phys. Rev. B **18**, 1 (1978).
[5] D. S. Gemmell, J. Remillieux, J. C. Poizat, M. J. Gaillard, R. E. Holland, and Z. Vager, Nucl. Instrum. Methods **132**, 62 (1976).
[6] W. Brandt and R. H. Ritchie, Nucl. Instrum. Methods **132**, 45 (1976).
[7] P. M. Echenique, R. H. Ritchie, and W. Brandt, Phys. Rev. B **20**, 2567 (1979).
[8] Y. N. Wang, Z. L. Mišković, and W. K. Liu, Phys. Rev. A **58**, 1287 (1998).
[9] Z. L. Mišković, W. K. Liu, and Y. N. Wang, Phys. Rev. A **57**, 1 (1998).
[10] H. B. Nersisyan and A. K. Das, Phys. Rev. E **62**, 5636 (2000).
[11] J. Jensen and P. Sigmund, Phys. Rev. A **61**, 032903 (2000).
[12] N. R. Arista, Nucl. Instrum. Methods Phys. Res. B **164/165**, 108 (2000).
[13] Z. L. Mišković, S. G. Davison, F. O. Goodman, W. K. Liu, and Y. N. Wang, Phys. Rev. A **63**, 022901 (2001).
[14] Z. L. Mišković, W. K. Liu, F. O. Goodman, Y. N. Wang, Phys. Rev. A **64**, 064901 (2001).
[15] T. Peter and J. Meyer-ter-Vehn, Phys. Rev. A **43**, 2015 (1991).
[16] J. D'Avanzo, M. Lontano, and P. F. Bortignon, Phys. Rev. E **47**, 3574 (1993).
[17] E. M. Bringa and N. R. Arista, Phys. Rev. E **54**, 4101 (1996).
[18] D. H. H. Hoffmann, R. Bock, A. Y. Faenov, U. Funk, M. Geissel, U. Neuner, T. A. Pikuz, F. Rosmej, M. Roth,

W. Süß, N. Tahir, and A. Tauschwitz, Nucl. Instrum. Methods Phys. Res. B **161/163**, 9 (2000).
[19] A. Sakumi, H. Okazaki, T. Watanabe, K. Shibata, H. Fukuda, U. Neuner, S. Garnsomsart, M. Ogawa, and Y. Oguri, Nucl. Instrum. Methods Phys. Res. A **415**, 648 (1998).
[20] U. Neuner, M. Ogawa, H. Kobayashi, M. Takizawa, K. Nishigori, A. Sakumi, M. Nakajima, K. Horioka, Y. Oguri, S. Miyamoto, and S. Garnsomsart, Nucl. Instrum. Methods Phys. Res. A **415**, 586 (1998).
[21] C. Deutsch *et al.*, Nuovo Cimento Soc. Ital. Fis., A **106A**, 1821 (1993).
[22] C. Couillaud, R. Deicas, Ph. Nardin, M. A. Beuve, J. M. Guihaumé, and M. Renaud, Phys. Rev. E **49**, 1545 (1994).
[23] N. R. Arista, R. O. M. Galvão, and L. C. M. Miranda, Phys. Rev. A **40**, 3808 (1989).
[24] I. Abril, A. Gras-Marti, and N. R. Arista, Nucl. Instrum. Methods Phys. Res. B **67**, 17 (1992).
[25] H. B. Nersisyan and E. A. Akopyan, Phys. Lett. A **258**, 323 (1999).
[26] C. Zhang, Solid State Commun. **116**, 241 (2000).
[27] C. Zhang and W. Xu, Physica B **298**, 333 (2001).
[28] C. A. B. Silva and R. M. O. Galvão, Phys. Rev. E **60**, 7441 (1999).
[29] Y.-N. Wang, H.-T. Qiu, and Z. L. Mišković, Phys. Rev. Lett. **85**, 1448 (2000).
[30] Y. H. Song, Y. N. Wang, and Z. L. Mišković, Phys. Lett. A **285**, 183 (2001).
[31] R. Kronig and J. Korringa, Physica (Amsterdam) **10**, 406 (1943).
[32] S. Lundquist, in *Theory of the Inhomogeneous Electron Gas*, edited by S. Lundquist and N. H. March (Plenum, New York, 1983).
[33] J. J. Dorado, O. H. Crawford, and F. Flores, Nucl. Instrum. Methods Phys. Res. B **93**, 175 (1994).
[34] A. Arnau and E. Zaremba, Nucl. Instrum. Methods Phys. Res. B **90**, 32 (1994).
[35] N. R. Arista, R. O. M. Galvão, and L. C. M. Miranda, J. Phys. Soc. Jpn. **59**, 544 (1990).
[36] Y. N. Wang, Y. H. Song, Z. L. Mišković, and W.-K. Liu, Nucl. Instrum. Methods Phys. Res. B **153**, 26 (1999).